Validity and Comparison between 2D (Normal Photo) and 3dMD (3D image) in Orthodontic Diagnosis

By

Amin Neishaboory

A thesis submitted to the Faculty of Graduate Studies of the University of Manitoba

in partial fulfillment of the requirements for the degree of

MASTER OF SCIENCE

(ORTHODONTICS)

University of Manitoba
Department of Preventative Dental Science
Division of Orthodontics
Winnipeg, Manitoba
Canada

Abstract

Objective:

The aim was to evaluate the validity and comparison between direct anthropometry measurements as the "Gold Standard" with 2D-images (Normal Photo) and 3D-images (3dMD) as a new contemporary tool for orthodontic diagnosis.

Methods & Materials:

51 subjects (22 Male and 29 Female) were randomly selected, without facial deformity, surgery or facial hair. Eight anatomical landmarks were selected and plotted on the face to create 7 linear and 4 angular measurements which were measured directly (D) by a digital caliper and a protractor (www.examobile.com).

Photos (2D) were taken with a Nikon DSLR camera and ring flash in NHP as well as a 3D-image with the 3dMD system (Atlanta, Georgia, USA). Both 2D photos and 3D images were analyzed by Tracker (www.opensourcephysics.org/Douglas Brown) and Vultus software for the same linear and angular parameters measured for each subject, respectively.

10% of the samples (5 cases) were randomly re-measured for intra-observer reproducibility. Collected data were analyzed by SAS using the paired t-test to compare the validity of direct (D), 2D and 3D measurements.

Results:

The results show no statistically significant difference between the direct measurement group (D) and 3D measurements. ($p > 0.05$) but a highly statistically significant difference is evident between the direct measurement group (D) and 2D measurements. ($p < 0.01$)

The 2D and 3D measurement groups also showed a statistically significant difference.($p < 0.05$)

Conclusion:

- ➤ This study has validated the accuracy of 3D measurements versus direct measurement.
- ➤ 3D measurement techniques are more accurate, almost by 1mm in linear and up to 1 degree in angular measurements, than 2D techniques.

Acknowledgments

- My supervising committee
  - Dr. Robert Drummond – Supervisor
  - Dr. William Wiltshire – Co-Supervisor
  - Dr. Kevin Vint – Internal Examiner
  - Dr. Adnan Shah – External Examiner

- All the staff, friends and colleagues at the Graduate Orthodontic Program.

Dedication

Every challenging work needs self-effort as well as guidance of elders, especially those who are very close to our heart.

My humble effort I dedicate to my sweet and loving

Father & Mother,

Also to my beautiful wife,

Roshi,

Whose affection, love, encouragement and prayers, day and night, made my work a success and honor.

Along with all hard working and respected

Teachers.

Table of Contents

<u>List of Tables</u>

List of Figures

1.Introduction

1.1. 3D Stereo Photogrammetry Technology

Orthodontic diagnosis requires a broad overview of the patient's situation and must take into consideration both objective and subjective findings (Proffit, Fields, and Sarver 2015).

It is a mistake for an orthodontist not to evaluate the face carefully (Proffit, Fields, and Sarver 2015).

The orthodontic profession is a specialty founded on the analysis and interpretation of geometries representing facial proportions. Dimensions and ratios are translated into representations of ideals and applied to facial aesthetics (Nanda et al. 2015).

The traditional foundation of orthodontics has relied on two-dimensional imaging to recreate the three-dimensional facial intricacies that exist in human anatomy (Nanda et al. 2015).

During the past decade, technological advancements have allowed visualization of bony anatomy and even more recently the soft tissues of the face (Nanda et al. 2015).

The orthodontic profession now has access to more information in three dimensions than ever before (Nanda et al. 2015).

It is our professional responsibility to utilize this information and apply these advancements in imaging towards improved diagnosis and patient care.

There is a strong need for investigations which analyze progress and change in three dimensions, to supplement and enhance traditional treatment modalities (Forst et al. 2014).

Although frontal and lateral cephalometric radiographs, panoramic radiographs, intraoral and extraoral photographs are still used widely, more emphasis is being placed on 3D virtual images and soft-tissue esthetics (Proffit, Fields, and Sarver 2015).

The soft tissue paradigm shift in treatment philosophy, also means that many clinicians have started to plan from the external profile, placing increased importance on the soft tissues of the face, largely to determine the limitations of orthodontic treatment.

From the perspectives of function, stability, and esthetics, the orthodontist must plan treatment within the patient's limits of soft-tissue adaptation and contours (Ackerman, Proffit, and Sarver 1999).

Three-dimensional facial photographic imaging was introduced to orthodontics during the early years of the millennium and may still be regarded to be in its infancy stages of development and implementation.

1.2. 3dMD image acquisition

The 3D information is obtained through the acquisition and comparison of a number of specific photographic images (Galantucci, Ferrandes, and Percoco 2006) that make use of the principle of triangulation, as shown schematically in Fig 1.

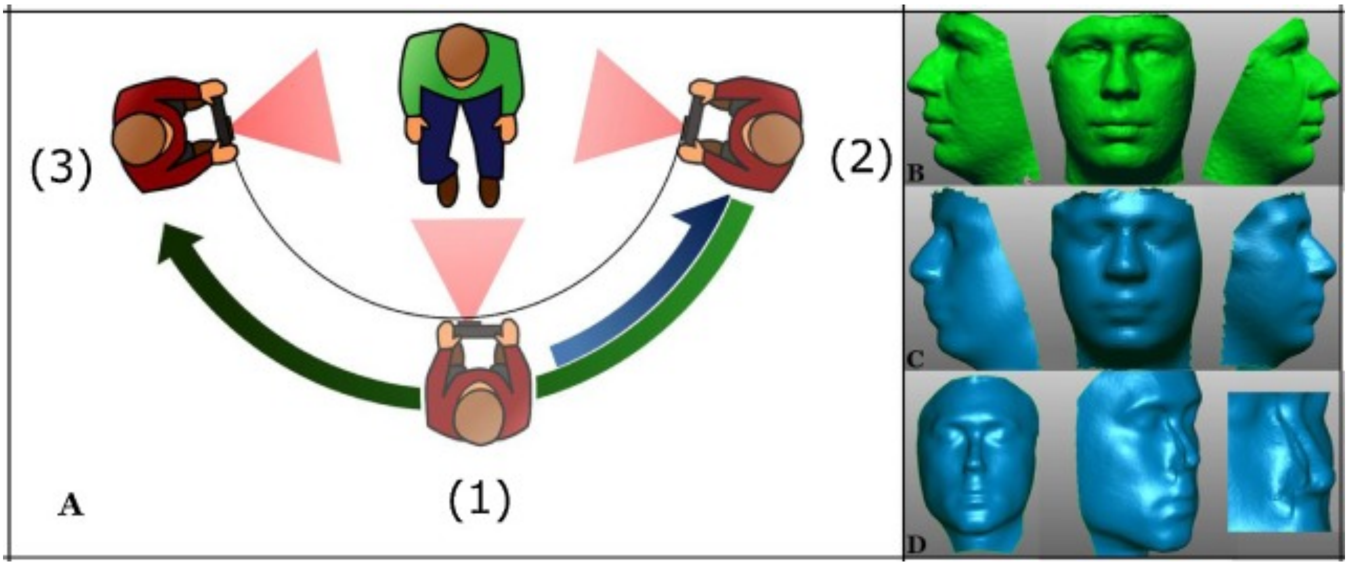

Fig 1. Triangulation principle (Maués et al. 2018).

High-resolution 3D scanning methods with an image capture time of a fraction of a second (2 milliseconds) which makes it resistant to motion artifacts, are now available. The apparatus (3dMD; 3Q, Inc) generates a 3D point cloud for analysis, and a software analytic system generalizes to the photogrammetric method.

The point cloud generated by the stereo-photogrammetry system is plotted in 3D space, and x, y, z coordinates are computed for the scanned surface by a software model that combines the geometry of a multiple-digital camera array and pre-calibrated distances to the subject with texture images from a color camera (3dMD; 3Q, Inc).

Each viewpoint overlaps and these are merged into a single 3D geometry. A circuit-board synchronizes the camera sensors, so that the images are integrated almost simultaneously, thus helping to minimize motion and lighting artifacts (3dMD; 3Q, Inc).

2.Literature Review

2.1. Fundamentals of 3D surface imaging technology

Two of the most popular techniques to create a three-dimensional image are structured-light and stereo-photogrammetry.

2.1.1. Structured-Light

Structured-light technology estimates the 3D surface of an object by the deformation of a projected pattern, with the knowledge about the design and geometry of a projected pattern and perception of the deformation by the 3D surface of the object, it is possible to estimate the 3D surface of the object and generate a 3D surface image (Fig 2) (Lane and Harrell 2008).

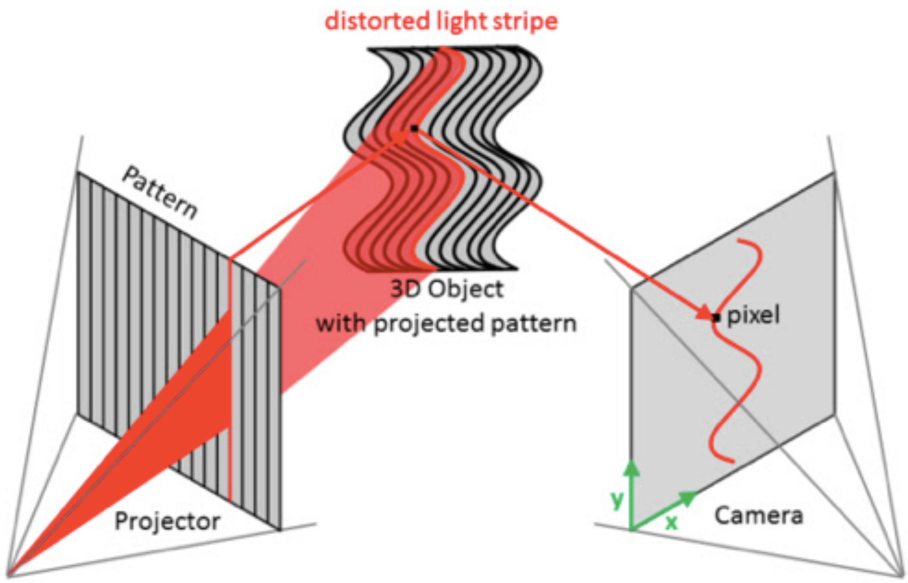

Fig 2. Structural-light projection (Lane and Harrell 2008).

2.1.2. Stereo-photogrammetry

Stereo-photogrammetry is based on structured light. There are three different strategies for stereo-photogrammetry: Active, Passive and Hybrid.

In "Active stereo-photogrammetry" it projects a pattern onto the surface of an object and uses two (or more) cameras to capture the deformations of the pattern by the objects' surface from different viewpoints.

A 3D surface image is generated by a process called "Triangulation", calculating the 3D coordinate of each 2D point (pixel) visible in both camera views.

This is achieved by combining the knowledge about the system (position of camera, distance of camera, etc.) and the captured 2D images of the cameras with their correspondences (pairs of 2D points/pixels, which occur in both camera views) (Fig 3) (Lane and Harrell 2008).

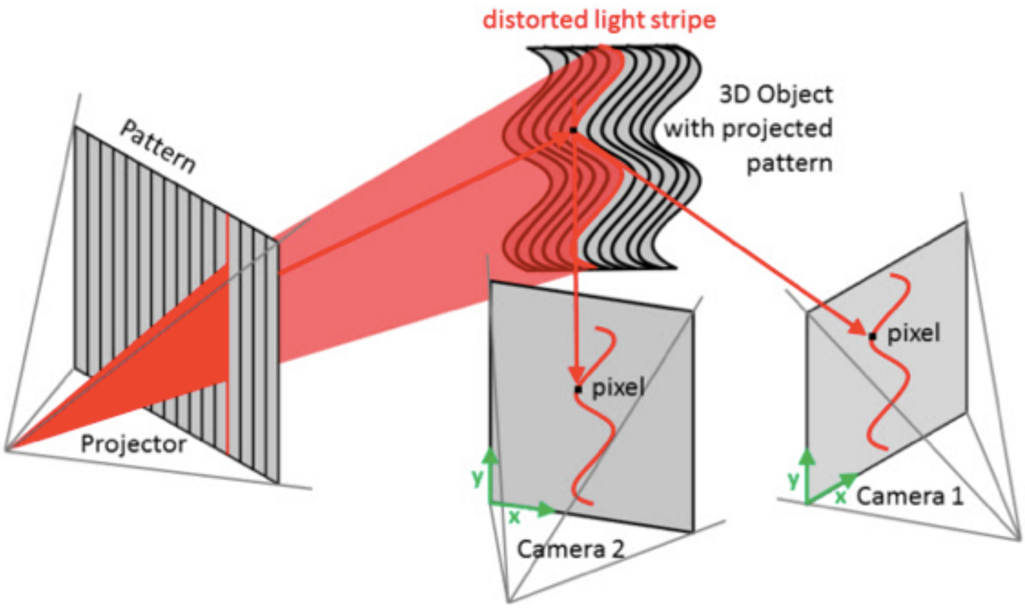

Fig 3. Active stereo-photogrammetry (Lane and Harrell 2008).

By contrast," Passive stereo-photogrammetry" determines 3D surface images only based on the images taken by two (or more) cameras without the projection of a pattern. Due to the missing projected pattern, the process of finding correspondences between views/images is more difficult and ambiguous (Fig 4) (Lane and Harrell 2008).

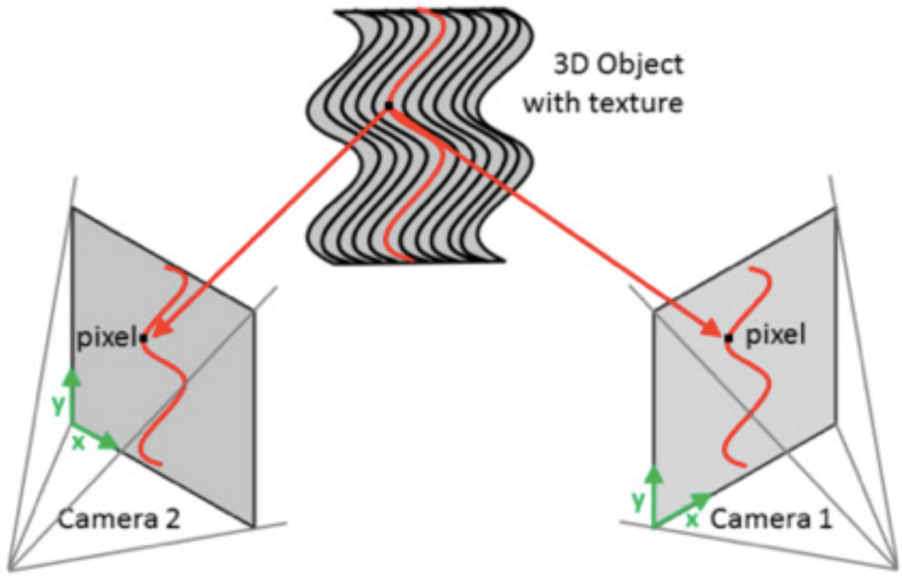

Fig 4. Passive stereo-photogrammetry (Lane and Harrell 2008).

To achieve a better image quality and higher accuracy, the new devices combined the active and passive technique, which is called Hybrid stereo-photogrammetry (Chae et al. 2016).

2.2. History of using 3D imaging for diagnosis

In the 1970s and 1980s, there was a growing awareness that the aesthetic outcome is of equal importance to the patient as the rearrangement of the occlusion. Methods of studying the facial profile or for planning surgical treatment were reintroduced, including facial plaster casts, anthropometry and analog photography (Arnett and Bergman 1993).

Digital photography was introduced to evaluate facial harmony. It allows clinicians to establish a more proportional focus on all three structures of the triad, to assess the patient's deformity (Arnett and Bergman 1993).

An accurate and objective assessment of facial deformity or preoperative prediction of the surgical outcome in two dimensions, especially regarding asymmetry, will always be deficient since it does not address the volumetric changes of all the facial portions, that determine neuromuscular balance and facial harmony (Arnett and Bergman 1993).

From the 1980s, the shortcomings of these techniques induced an increase in the use of three-dimensional (3D) imaging techniques, to render the facial soft tissue surface (Arnett and Bergman 1993).

2.3. Current Studies

The accuracy and reliability of 3D measurements of facial soft tissues were evaluated through comparisons of data obtained on the same sample of subjects using 3D computer tomography and 3D stereo-photogrammetry (Swennen et al. 2005).

The measurement of the facial soft tissue with 3D computer tomography showed great accuracy, except for the landmarks of the hairline, the eyebrows, and the eyelids (Naini et al. 2017).

In contrast, 3D stereo-photogrammetry showed great accuracy and reliability, except for the bony landmarks. Thus, the combination of 3D computer tomography and 3D stereo-photogrammetry for the analysis of facial soft tissue allows these problems related to the hairline, eyebrows, eyelids, and the bony landmarks to be overcome (Swennen et al. 2005).

The study of Ghoddousi and co-workers compared the accuracy of the mapping of facial soft tissue using 3D stereo-photogrammetry, manual anthropometric measurements, and 2D photographs and found that there are no significant differences between them (Ghoddousi et al. 2007).

Rangel et al. presented a study using the 3dMD (Atlanta, GA, USA) stereo-photogrammetric system where they obtained a 3D digital model having an average error of 0.35 mm with a standard deviation of 0.32 mm (Rangel et al. 2008).

Khambay et al. validated a high-resolution 3D imaging system (Di3DTM, Dimensional Imaging Ltd., Glasgow, Scotland, UK) using only ten landmarks on facial plaster casts, comparing the results with those obtained by a coordinate-measuring machine (CMM) and reported a system error of 0.2 mm and a reproducibility error of less than 0.5 mm (Khambay et al. 2008).

Winder and his co-workers used 18 landmarks on a mannequin head to validate a Di3DTM system, using comparison laser scans and digital caliper measures. Mean differences between the measurements of 0.62 mm were shown (Winder et al. 2008).

In 2010, Lübbers et al. examined the precision and accuracy of the 3dMD system using 41 landmarks on a mannequin head; they report a mean global error of 0.2 mm (range 0.1 to 0.5mm).

More recently, Hellak et al. repeated the experiments using 61 landmarks on two real faces, reporting a mean global error of 0.41 mm (range 0 to 3.3 mm) (Hellak et al. 2015).

Deli and team compared the results achieved with various photogrammetric systems and they found different numbers with different types of cameras (Deli et al. 2013).

Galantucci et al. recently also developed a simple photogrammetric system for automatic capture and measurement of facial soft tissues during movement. They suggested that digital close-range photogrammetry be used to acquire the spatial coordinates of facial landmark points and track their movements, which showed good repeatability of measurements (Galantucci, Ferrandes, and Percoco 2006).

The most current methods for analyzing the 3D photographic images involve simple visual evaluation of linear and angular measures between various point landmarks to evaluate facial aesthetics and proportions (Naini et al. 2017).

3.Purpose

The aim of this study was to evaluate the validity and comparison between direct anthropometry as the "Gold Standard" with 2D and 3D photogrammetry to establish 3D images as a potential contemporary tool for orthodontic diagnosis.

4.Null Hypothesis

- There is no significant difference between the direct (D) and 2D measurements.
- There is no significant difference between the direct (D) and 3D measurements.
- There is no significant difference between 2D and 3D measurements.

5.Methods and Materials

5.1. Ethics Approval:

Approval was obtained from Ethics Board Committee of the University of Manitoba, following which the participants were informed verbally and in writing and volunteer consent forms signed by all participants.

5.2. Sample group and size:

The study was conducted with 51 randomly selected subjects (22 Male and 29 Female) with an age range of 19-26/yr. The sample comprised of dental students at the Dental College of the University of Manitoba. For an effect size at a 0.05 significance level, it was determined that greater than 95% power could be achieved with a sample size of 50.

After a brief introduction of the project to each participant and the exclusion criteria applied, an informed consent form was signed.

An identification code (A1-A51) was allocated for each subject.

5.3. Exclusion Criteria:

- No facial deformity.
- No facial cosmetic surgery/procedure.
- No facial hair.
- No significant facial asymmetry.

Data collected in three categories:

- Direct measurements.
- A set of 2D images. (Frontal and Profile)
- A set of 3D images.

5.4. Photo acquisition protocol:

The 2D and 3D images were acquired within the same day at the Orthodontic Clinic of the College of Dentistry, University of Manitoba.

2D and 3D images were acquired, and then direct measurements were performed following markings on the face.

5.4.1. 2D photos:

Two vertical mirrors were mounted on the wall in front of the subjects at their eye level and they were instructed to look at their eyes for both frontal and profile photos to achieve natural head position (NHP) before photo shooting.

To prevent any shadow on the images, a mounted fluorescent light-box was used as the background and a 50-millimeter ruler was mounted on the top right corner of the light-box which was used for calibrating the software and avoid magnification errors.

Frontal and profile photographs of the participants were captured under the same illumination using a professional DSLR camera (Nikon D3200 24.2-megapixel DX,

Tokyo, Japan) with a professional Micro Nikkor lens (AF-S Micro Nikkor 85mm 1:3.5 G ED, Tokyo, Japan) which was placed on a tripod in the focal zone away from the participant.

The same identification coding system (A1-A51) was used for all the photographs and they were transferred to a computer and calibration procedures were then performed using Tracker software 4.11.0 (Tracker www.opensourcephysics.org, Douglas Brown).

Seven linear and four angular measurements were made on each image (Table 2 & 3).

All the images were acquired by positioning the participants in the same position as in the direct measurement method.

5.4.2. 3D photos:

The 3dMD system from Atlanta, Georgia, USA was used for the 3D image acquisition. The machine was calibrated according to the manufacturer instructions, every day before each photo shoot.

Participants were positioned in the calibrated zone on an adjustable seat for the 3D image acquisition.

A 3D image was created, an identification code allocated (A1-A51) and saved on the 3dMD Face software (Vultus) for further analyzing.

Seven linear and four angular measurements were made on each image (Table 2 & 3).

5.5. Measurement protocols:

Direct measurements were made on the day of image acquisition.

Measurements of the 2D and 3D images were made in a randomized manner and on a different day from the direct measurements.

5.5.1. Landmarks and definitions:

8 anatomical landmarks on the face were plotted according to the table below (Table 1-Fig 5).

Landmarks	Abbreviation	Definition
Nasion	Na	The outer point of intersection between the nasion-sella line and the soft tissue profile.
Subnasal	SubN	A point on the living where the nasal septum and the upper lip meet in the midsagittal plane
Columella	Col	The bridge of tissue that separates the nostrils at the nasal base
Pogonion	Pog	The most anterior mid- point of the chin.
Upper vermilion	UV	Upper border on upper lip vermilion
Tragus	Trg	The most posterior part of the external meatus of the ear.
Cheilion	Ch	The point located at each labial commissure.
Ala of the nose	Ala	The most lateral point on each alar contour.

Table 1: Landmarks and definitions.

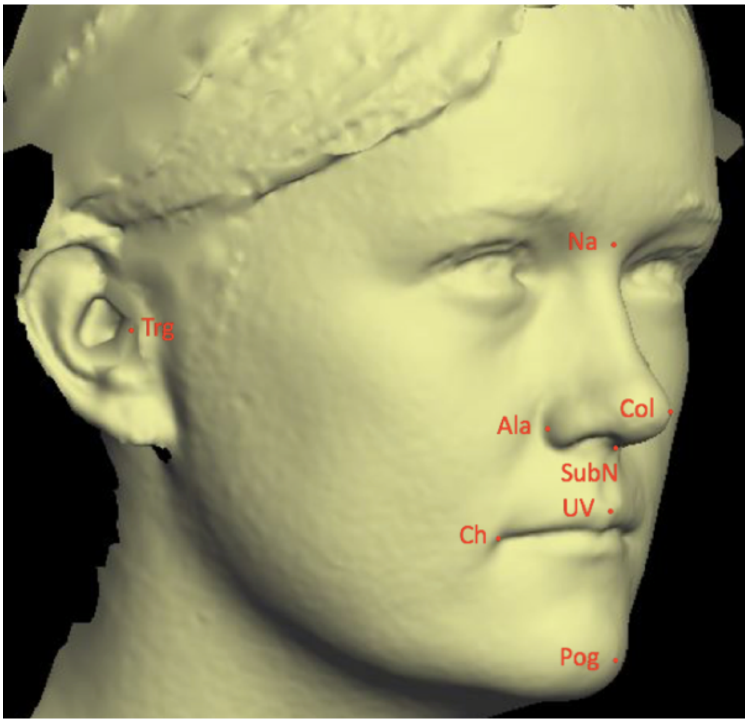

Fig 5. Anatomical landmarks.

5.5.2. Linear parameters and definitions:

A set of 7 linear variables created and defined according to the table below (Table 2 - Fig 6,7).

Abbreviation	Landmarks	Definition
SbN-UV	SbN, Upper Vermelion. (mm)	Vertical linear measurement from SbN to the border of upper lip vermelion
Ch-Ch	Cheilion right, cheilion left. (mm)	Transverse linear measurement of mouth width from Cheilion right (Ch-R), to Cheilion left (Ch-L)
Al-Al	Alare right, Alare left. (mm)	Transverse linear measurement of nasal width from Alare right to Alare left.
Tr-SbN	Tragus, Subnasale. (mm)	Sagittal linear measurement from Tragus to Subnasale
Tr-Pog	Tragus, Pogonion. (mm)	Sagittal linear measurement from Tragus to Pogonion
N-SbN	Nasion, Subnasale. (mm)	Vertical linear measurement of mid-face from Nasion to Subnasale
Sn-Pog	Subnasal, Pogonion. (mm)	Vertical linear measurement of lower facial dimension as measured from Subnasale to Pogonion

Table 2: Linear parameters and definitions.

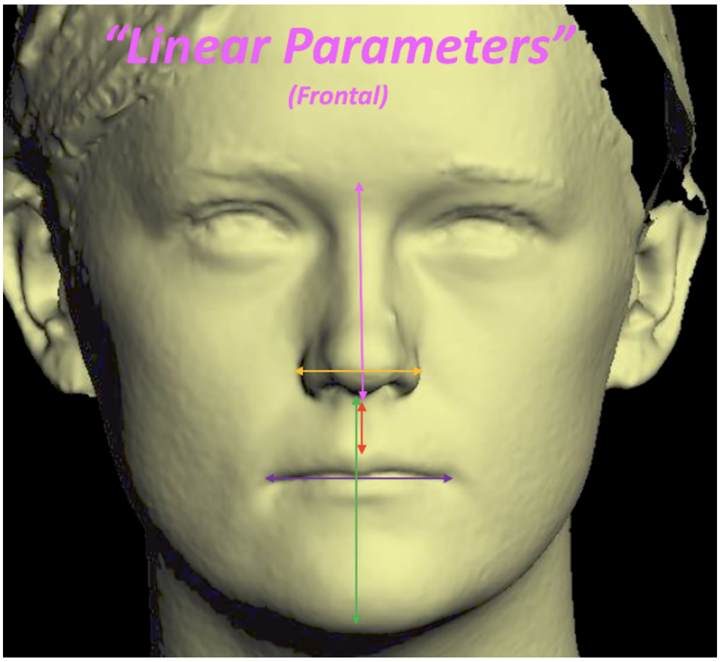

Fig 6. Frontal linear measurements.

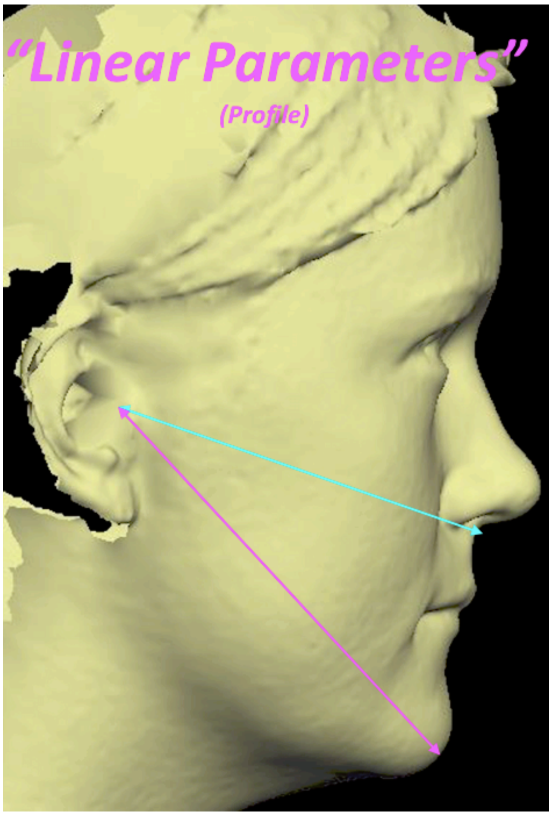

Fig 7. Profile linear measurements.

5.5.3. Angular parameters and definitions:

A set of 4 angular variables created and defined according to the table below (Table 3-Fig 8,9).

Abbreviation	Landmarks	Definition
NLA (Col-SbN-LS)	Columella. Subnasale, Labium superior (°)	Angular measurement from Columella to Subnasale to Labium superior (nasolabial angle)
N-Tr-SbN	Nasion, Tragus, Subnasale (°)	Angular measurement from Nasion to Tragus to Subnasale (angle of medium facial third)
SbN-Tr-Pog	Subnasale, Tragus, Pogonion (°)	Angular measurement from Subnasale to Tragus to Pogonion (angle of inferior facial third)
N-SbN-Pog	Nasion, Subnasale, Pogonion (°)	Angular measurement of soft tissue profile from Nasion to Subnasale to Pogonion

Table 3: Angular parameters and definitions.

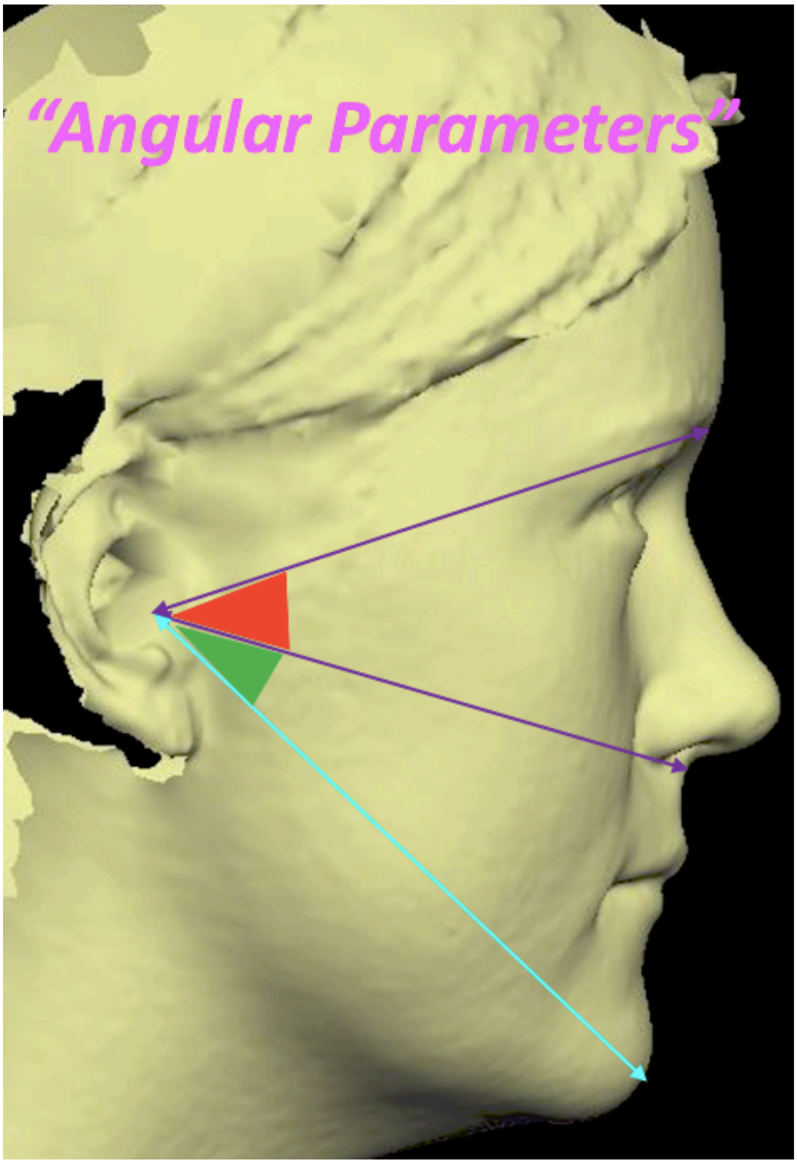

Fig 8. Upper and Lower Facial angle.

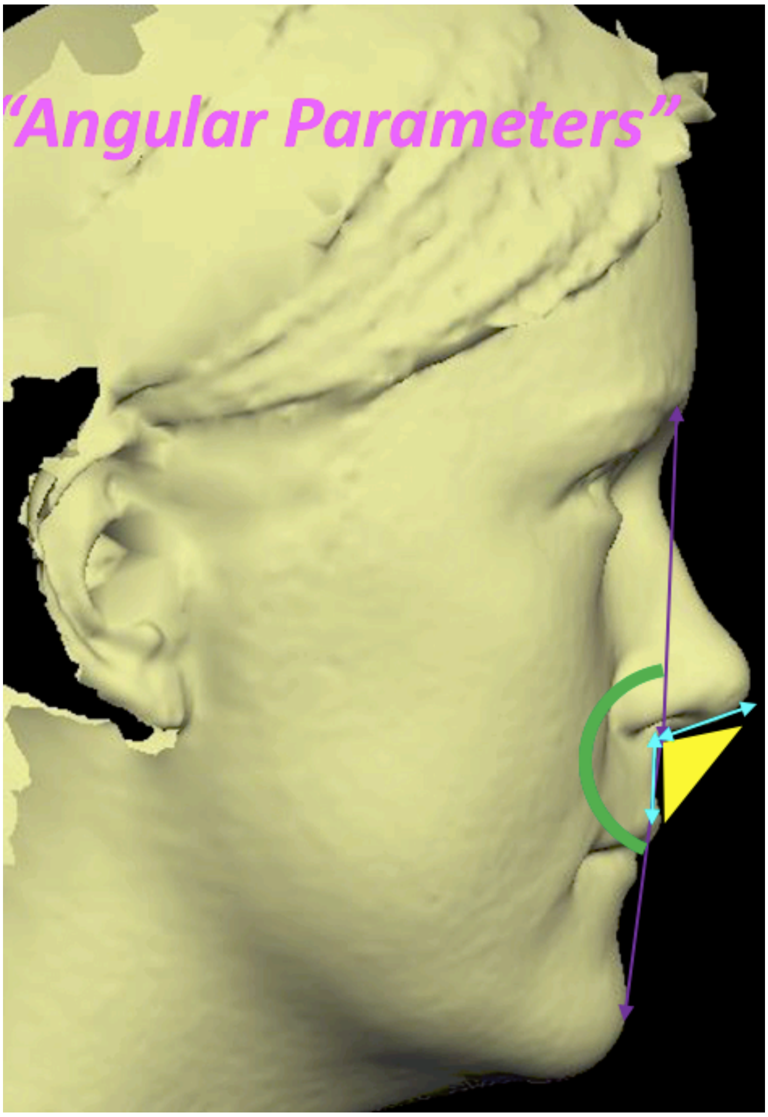

Fig 9. NLA and Facial Convexity.

5.5.4. Direct measurements:

Anatomical points required for linear measurements were determined by inspection and palpation, then marked on the face.

A fine 0.5mm eye-liner was used to mark the face of the subjects according to "Table 1".

During the determination and measurement of the points, it was ensured that the subjects were relaxed and seated with a natural head position and relaxed lips.

5.5.4.1. Linear direct measurement:

To measure the linear variables, a digital millimeter sliding caliper used. The caliper was adapted on the skin over the plotted landmarks to measure the linear distance between the two nominated landmarks for linear variables (Table 2).

The digital caliper was set on millimeter (mm) and set at zero for each measurement.

Extracted linear parameter data for the direct group were imported and saved into an excel sheet (Appendix, Table 4).

5.5.4.2. Angular direct measurement:

A digital protractor software (www.examobile.com) was installed on a smartphone (i-phone 8) and the device mounted on a bench with a fix-screwed holder within a 35cm distance from the subject's face, according to the manufacturer's instructions at the best focal spot.

The angular parameters for the direct group were measured and extracted data, saved into an excel sheet (Appendix, Table 5).

5.5.5. 2D measurement technique:

Both 2D photographs (frontal & profile) for each subject were imported into Tracker software (www.opensourcephysics.org, Douglas Brown 4.11.0) and the landmarks were plotted according to (Table 1).

Tracker software was calibrated according to the manufacturer's instructions by using the 50mm mounted tape measure from the background of each of the photos to achieve the most accuracy in the measurements.

Landmarks were connected and measurements were performed for both linear and angular variables according to tables 2 and 3.

The extracted results from the Tracker software for both linear and angular measurements were saved in an excel sheet as (2D-linear) and (2D-Angular) variables (Appendix, Table 6 -7).

5.5.6. 3D measurement technique:

3D images were plotted, according to (Table 1) for each subject in 3 planes of space (x, y, z) on Valtus software from 3dMD following the manufacturer's instructions.

Plotted landmarks to extract the linear and angular variables according to (Table 2 &3).

Data for both linear and angular measurements from Valtus software were saved in an excel sheet as of (3D-linear) and (3D-angular) measurements (Appendix, Table 8 - 9).

Note: IDs for each case were kept the same in all the 3 different measurement groups (ID: A1- A51 for D- 2D- 3D).

5.6. Reliability protocols:

5.6.1. Intra-examiner reliability:

To evaluate the intra-observer agreement, 10% of the sample pool was selected randomly by selecting 5 numbers among 1-51 from a hat draw and all the 3 measurements (D, 2D, and 3D) were then performed on randomly selected subjects, 1 week after finishing data collection from the main subject pool with the same standards as the first attempt for data collection which is described above (Appendix, Table 10).

Intra-observer agreement for the D, 2D and 3D method was evaluated similarly using the Paired t-test, to indicate the Intra-class Correlation Coefficient (ICC).

5.6.2. Inter-examiner reliability:

As the aim was not to evaluate the diagnostic ability of the investigator, there was no need to have an inter-examiner reliability test, according to the statistician's recommendation.

5.7. Methods of Comparison:

Comparison was conducted statistically on 11 parameters (7 linear – 4 angular) between 3 groups (D – 2D), (D – 3D) and (2D – 3D).

Direct measurement is considered as the "Gold Standard".

5.7.1. Comparison between direct (D) and 2D groups:

All the 11 parameters in the 2D group were compared with the direct measurements (Gold Standard), to determine the reliability based on the mean differences between each variable.

5.7.2. Comparison between direct (D) and 3D groups:

All the 11 parameters in the 3D group were compared with the direct measurements (Gold Standard), to determine the reliability based on the mean differences between each variable.

5.7.3. Comparison between 2D and 3D groups:

Comparison was conducted between the 2D and 3D groups, to evaluate their validity, based on the mean differences between each variable.

5.8. Statistical Analysis:

All statistical analyses were performed using the SAS System (D.17 Statistical Analysis System) version 9.3 software (SAS Institute Inc., Cary, North Carolina, USA). Normal distribution of the data was evaluated using the Shapiro-Wilk test.

The direct measurement (D) was considered as the “Gold Standard”, so the extracted data for 2D and 3D were compared with the extracted data from the direct group (D), for both linear and angular measurements by using Paired t-test.

The Paired t-test was used to determine the significance of the differences between the direct measurement group (D), photogrammetry (2D), and 3D stereo-photogrammetry.

In this study statistical comparison was conducted on 11 parameters (7 linear – 4 angular) between 3 pairs; (D – 2D), (D – 3D) and (2D – 3D) by 33 Paired t-tests.

To adjust the P-value ($P = 0.05$), Bonferroni Correction was used to correct the inflated type I error due to Multiple Paired t-tests by the number of each Paired t-tests ($n = 33$). ($P^* = P \div 33 = 0.0015$)

Intra-class correlation coefficient (ICC) was used to evaluate the agreement between the measurements based on 10% of randomly selected subjects.

6. Results

6.1. Comparison between direct (D) and 2D groups:

A highly statistically significant difference is evident between the direct measurement group (D) and the 2D measurements. ($p < 0.01$)

All the differences observed between means were > 1mm and >1 ° for all the parameters (Table 11).

		D-2D	
	Mean	**Mean Difference (95% CI)**	
Linear		**Lower 95%**	**Upper 95%**
Sn-U Ver	0.72	0.58	0.86
Ch-Ch	0.31	0.13	0.49
Al-Al	-0.66	-0.86	-0.47
Tr-Sn	1.1	0.81	1.39
Tr-Pog	0.88	0.7	1.05
N-Sn	-0.72	-0.9	-0.54
Sn-Pog	1.01	0.86	1.15
Angular			
NLA	-0.72	-0.89	-0.56
N-Tr-Sn	-0.87	-1.04	-0.7
Sn-Tr-Pog	-0.95	-1.14	-0.76
N-Sn-Pog	1.2	1.02	1.37

Table 11: Mean differences between D - 2D.

6.2. Comparison between direct (D) and 3D groups:

The results show no statistically significant difference between the direct measurement group (D) and the 3D measurements. ($p > 0.05$)

Both linear and angular mean differences reported < 1mm and < 1°, respectively (Table 12).

		D-3D	
	Mean	***Mean Difference (95% CI)***	
Linear		***Lowr 95%***	***Upper 95%***
Sn-U Ver	0.01	-0.09	0.12
Ch-Ch	0.06	-0.06	0.19
Al-Al	0.1	-0.02	0.23
Tr-Sn	0.13	0	0.27
Tr-Pog	-0.02	-0.18	0.12
N-Sn	0.17	0.03	0.31
Sn-Pog	0.16	0	0.31
Angular			
NLA	0.26	0.1	0.42
N-Tr-Sn	0.15	0.03	0.27
Sn-Tr-Pog	0.09	-0.04	0.24
N-Sn-Pog	0.2	0.05	0.34

Table 12: Mean differences between D - 3D.

6.3. Comparison between 2D and 3D groups:

The measurements between the 2D and 3D groups showed a statistically significant difference. ($p < 0.05$), with all the mean differences found > 1mm and > 1 ° for all the parameters (Table 13).

		2D-3D	
	Mean	**Mean Difference (95% CI)**	
Linear		**Lower 95%**	**Upper 95%**
Sn-U Ver	-0.71	-0.81	-0.61
Ch-Ch	-0.24	-0.38	-0.11
Al-Al	0.77	0.66	0.87
Tr-Sn	-0.96	-1.24	-0.68
Tr-Pog	-0.91	-1.01	-0.8
N-Sn	0.89	0.78	1
Sn-Pog	-0.85	-0.94	-0.76
Angular			
NLA	0.98	0.88	1.08
N-Tr-Sn	1.02	0.92	1.13
Sn-Tr-Pog	1.05	0.95	1.14
N-Sn-Pog	-1	-1.13	-0.86

Table 13: Mean differences between 2D - 3D.

6.4. ICC results:

The Reliability Coefficient (ICC) between the different methods were evaluated using the Paired t-test.

The results were determined to be statistically acceptable (ICC > 0.7) at an arbitrary value of 1 mm and 1 ° between first and second observations.

6.5. Results Summary:

In summary (Table 14), the results show no statistically significant difference between the direct measurement group (D) and 3D measurements. ($p > 0.05$) but a highly statistically significant difference is evident between the direct measurement group (D) and 2D measurements. ($p < 0.01$)

The 2D and 3D measurement groups also showed a statistically significant difference. ($p < 0.05$)

	D-2D			D-3D			2D-3D		
	Mean	Mean Difference (95% CI)		Mean	Mean Difference (95% CI)		Mean	Mean Difference (95% CI)	
Linear		Lower 95%	Upper 95%		Lowr 95%	Upper 95%		Lower 95%	Upper 95%
Sn-U Ver	0.72	0.58	0.86	0.01	-0.09	0.12	-0.71	-0.81	-0.61
Ch-Ch	0.31	0.13	0.49	0.06	-0.06	0.19	-0.24	-0.38	-0.11
Al-Al	-0.66	-0.86	-0.47	0.1	-0.02	0.23	0.77	0.66	0.87
Tr-Sn	1.1	0.81	1.39	0.13	0	0.27	-0.96	-1.24	-0.68
Tr-Pog	0.88	0.7	1.05	-0.02	-0.18	0.12	-0.91	-1.01	-0.8
N-Sn	-0.72	-0.9	-0.54	0.17	0.03	0.31	0.89	0.78	1
Sn-Pog	1.01	0.86	1.15	0.16	0	0.31	-0.85	-0.94	-0.76
Angular									
NLA	-0.72	-0.89	-0.56	0.26	0.1	0.42	0.98	0.88	1.08
N-Tr-Sn	-0.87	-1.04	-0.7	0.15	0.03	0.27	1.02	0.92	1.13
Sn-Tr-Pog	-0.95	-1.14	-0.76	0.09	-0.04	0.24	1.05	0.95	1.14
N-Sn-Pog	1.2	1.02	1.37	0.2	0.05	0.34	-1	-1.13	-0.86

Table 14: Mean differences between D - 2D -3D

The highest mean difference for the linear and angular measurements were 1.1mm and 1.2 ° respectively which were both found between the D and 2D groups.

Table 15, shows the highest mean differences between all 3 compared groups.

Comparison	Linear	Angular
D-2D	1.1 mm	1.2 °
D-3D	0.17 mm	0.26 °
2D-3D	0.89 mm	1.05 °

Table 15: The highest mean difference for the linear and angular measurements.

7. Discussion

7.1. Discussion

Conventional methods for studying facial symmetry have limitations. Radiography measures skeletal landmarks but ignores the aesthetic aspects of soft tissue. The 3dMD face system allows the collection of images stored in digital format.

In the current study, data acquisition was performed in natural head posture, because Kau et al (2005), were able to show that this position is clinically reproducible. Hence, the quality of the produced three-dimensional model represented was matched to reality with the least possible bias (Brons et al. 2012).

Concerning operator error, the zoom was used whenever the operator was in any doubt about a landmark, but this was not used as a routine. Even if the operator error could be reduced by using the zoom facility of the software, this strategy was deemed unnecessary because of the negligible error produced, even without the zoom feature, as our research showed the margin of error is from 0.1 to 0.04 mm.

For reliability, it is very important to have a clear acquisition of the facial regions to be measured. In the present study, images were acquired using nine modular units (Right: three, Left: three, Front: three) in order to avoid image loss all over the face, including the ear region.

We found the error of recalibration of the system (about 0.01 mm, according to the manufacturer), is negligible in itself and especially in comparison to the operator error, which is about 10 times higher.

In this project, we considered that the error resulting from the object's position is about the same magnitude as the operator error and in itself, is negligible for clinical applications.

Another point of discussion is the accuracy and bias compared with direct anthropometry. The distances directly measured and the distances calculated from the data sets revealed no relevant differences and therefore no imminent error that would lead to systematically incorrect results. However, performing the direct measurement was found to be more challenging than 3dMD, due to the geometry and the nature of the face.

Overall, however, the system error of the 3dMD system is comparable to that of other three-dimensional imaging systems (Naini et al. 2017).

Evaluating the properties of facial soft tissue clinically and quantitatively is a priority of contemporary orthodontic diagnosis and treatment planning. Many imaging techniques have been used to evaluate facial soft tissues, but 3D stereophotogrammetry has attracted more attention recently, because of the many advantages it has such as no radiation, high accuracy, easy to acquire, less time consuming, etc.

This method has been found to be accurate and reliable enough to be integrated into clinical orthodontic practice. Furthermore, it is possible to process and analyze 3D stereo-photogrammetric images in different software packages in accordance with the different clinical or research purposes.

Quantitative evaluations that are performed on facial soft tissues, in addition to clinical evaluations, are important for assessing treatment aims and treatment outcomes.

CBCT can be used for soft tissue analysis three-dimensionally, but it has several disadvantages. Besides the measurement difference between CBCT and 3D stereophotogrammetry was clinically insignificant. Accordingly, the use of stereophotogrammetry is considered adequate in the imaging of soft tissues and the measuring facial soft tissues (Forst et al. 2014).

Although the direct anthropometry method is not routinely used in clinical practice, it is nonetheless the most reliable method to evaluate the real measurements. This project used direct measurement as the gold standard to evaluate and compare with the other two measurements (2D and 3D) techniques.

The present study which evaluated the accuracy and reliability of 3D stereo-photogrammetry found a very high level of agreement between direct anthropometry, which is the gold standard, and 3D stereophotogrammetry.

This study found these values were considered to be clinically important but not significant, however, Dindaroğlu et al, 2016 claimed these are clinically significant (Dindaroğlu et al. 2016).

In the literature (Khambay et al 2009, Lübbers et al 2010 and Naini et al 2017), there are many reports that claim some discrepancy between direct and 3D measurement techniques, however, their results are based on analyzing the results that were achieved by comparing the data between different observers. However, in this research project, the main focus was on comparing different techniques (D-2D and 3D) by excluding/minimizing the observer/human errors.

The ability and accuracy of 3dMD machine to create such a precise image, which will minimize the percentage of operator errors is not the reason for this disagreement. However, disagreement could be the result of other factors such as different observers performing the same measurements, which will affect the results due to different interpretations of plotting the landmarks, patient positioning, image distortion/magnification, and the image quality.

Kochel et al. 2010 confirmed deviations are mostly caused by observer errors during placement of anthropometric points (Kochel et al. 2010).

In the present project, one of the most important factors was the reproducibility of the points determined for measurements. In fact, the low-range of variation in the present study is believed to have resulted from minor deviations that occurred during the placement of the morphologic points.

To eliminate interpretation discrepancies of the landmarks, the current project used the data generated by one operator to be able to compare the techniques without the introducing human errors.

In the literature, many imaging techniques have been used to evaluate facial soft tissues and this study is in agreement that 3D stereo-photogrammetry has many advantages, for soft tissue assessment (Lübbers et al. 2010), (Tzou and Frey 2011), (Naini et al. 2017).

Our study was in agreement with Lübbers et al (2010) and Khambay et al (2009) who examined the precision and accuracy of 3D stereo-photogrammetry and reported a mean global error between 0.1 and 0.5 mm (Lübbers et al. 2010).

The current research, also found the highest mean difference was 0.17mm in the linear and 0.26° in the angular measurements, which was in contrast with other published studies (Wong et al (2008), Winder (2008) and Metzger (2013)) who found a 2mm mean difference between 3D and direct measurements for the linear measurements and did not report any comparisons for the angular parameters (Wong et al. 2008).

The literature, based on statistical analysis alone, suggests that the intraclass correlation coefficient (ICC) > 0.7, (at an arbitrary value of 1 mm and 1 ° between first and second observations), is considered as statistically acceptable, which is in agreement with our study, where the results with ICC were between 0.95 and 0.99. This is deemed to be statistically acceptable even with a narrower margin for both the linear (0.17 mm) and angular (0.26 °) values.

The present study found the plotting of the face, for the measurements, in all the techniques (D-2D, and 3D), to be a challenging task that can affect the accuracy of the outcome. However, we found that the level of difficulty within different landmarks varies, based on several factors such as: unilateral (mid-line) or bilateral landmarks, techniques for the assessment (D,2D, and 3D), operator ability and the quality of the images.

Our results show that the majority of the errors occur for the unilateral (mid-line) landmarks, which is due to the nature of the techniques used for these measurements.

We believe, the geometry of the face, in the direct technique, and the lack of the third plane of space in the 2D technique, are the main reasons for inaccuracy. This study found the 3D technique, to be the most accurate technique, which gives the operator the ability to assess a particular landmark in the 3 planes of space.

Aldridge et al. (2010) reported that the greatest and most significant difference was 1.42 mm in the N-Prn (Nasion – Pronasale) measurement for interobserver agreement. However, the difference was 2 mm for all other parameters (Schimmel et al. 2010).

Wong et al 2008 found the grand mean of the precision calculated across subjects along with all axes for all landmarks was 0.827 mm (Wong et al. 2008).

Also, Plooij et al. found the highest interobserver agreement was in the Al-Al measurement (95% CI, 0.17 mm) (Naini et al. 2017).

Deli et al 2013, claimed interobserver agreement above 0.8 in most points with 1mm differences (Deli et al. 2013).

These findings are not consistent with our results for the linear measurements in the 3D technique. We believe the main reason for this inconsistency is due to the comparison of two techniques by different observers, however, in the current study only one observer performed the comparisons, to minimize the human errors.

However, this study and Aldridge et al (2010) were in agreement that mid-line landmarks, such as Nasion and Pronasale, are the most difficult landmarks to identify.

Farkas et al. (1994) reported that the difference between direct anthropometry and 2D photogrammetry may be caused by the distortions in photogrammetry. The experience in this study shows that finding some facial landmarks on 2D photos cannot be done accurately due to the geometry and 3-dimensional nature of the face. This issue becomes more problematic when dealing with unilateral (mid-line) anatomical landmarks (Fig. 10).

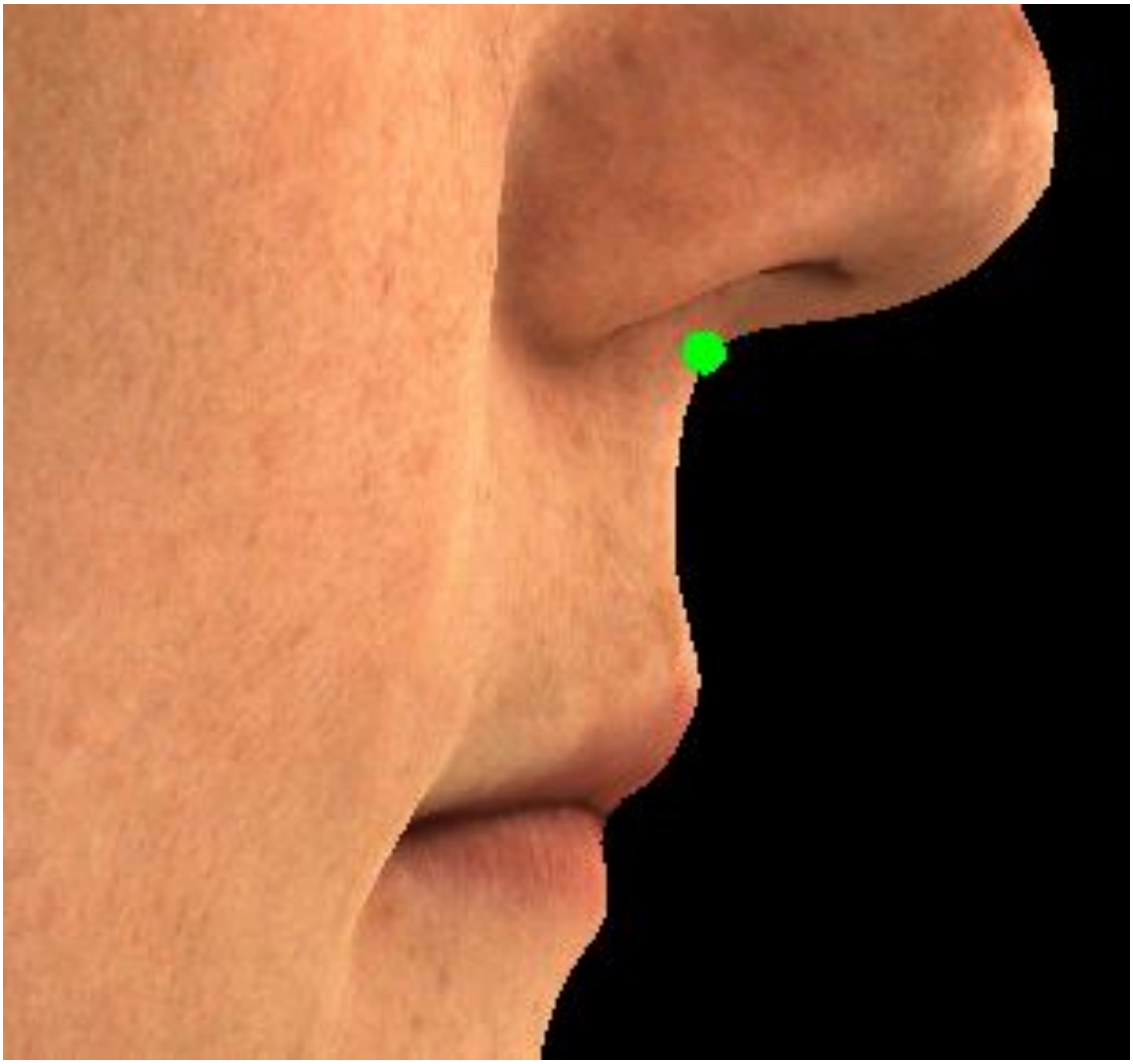

Fig 10. Sub-Nasale in 2D profile view.

Plotting a mid-line landmark on a 2D photo excludes the transverse dimension from the three planes of space, hence, the plotted spot misses its accuracy (Fig. 11).

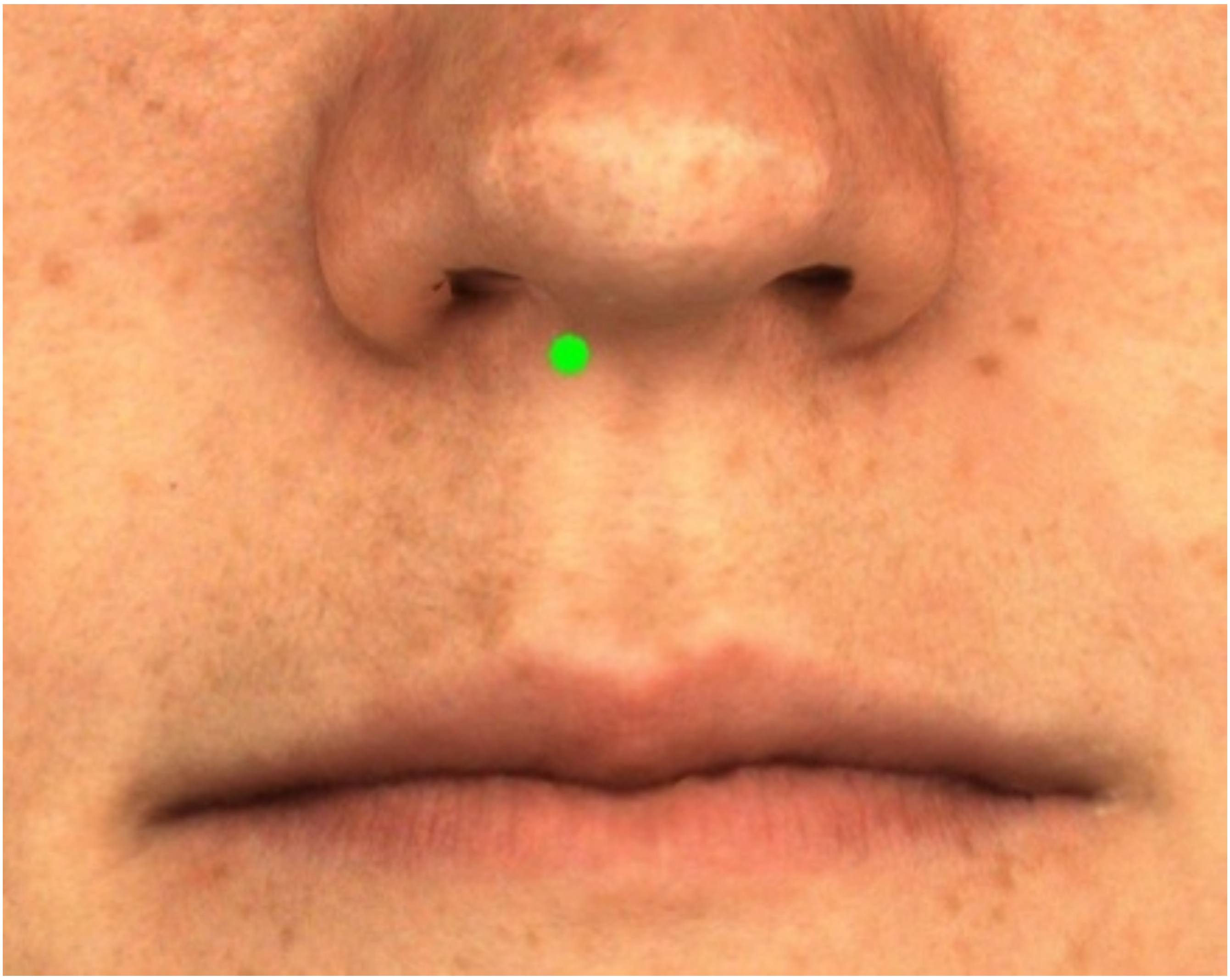

Fig 11. Sub-Nasale in 2D profile view.

3dMD Valtus software can show the error and inaccuracy of the selected spot for mid-line landmarks such as Sub-Nasale by evaluating the same image when moved to frontal aspect (Fig 12).

Fig 12. Sub-Nasale in 3D submental view.

Images produced by 3dMD give the ability to the clinician to assess the image in three planes of space, accurately select the right spot and plot the mid-line landmark in its correct location.

The present study found agreement between 2D photogrammetry and direct measurement techniques, however, this agreement was not as reliable/accurate as 3D techniques and direct measurements. Hence, this research indicates that 2D measurements can be used safely in soft tissue image analysis if the required accuracy is not less than 0.5mm. Thus, this technique (2D) is still reliable for clinical use, but with a lesser level of accuracy.

7.2. Null Hypothesis Evaluation:

- The first null hypothesis states that there is no significant difference between the direct (D) and 2D measurements.

This null hypothesis is **rejected** because a highly statistically significant difference is evident between these groups ($p < 0.01$).

- The second null hypothesis states that there is no significant difference between the direct (D) and 3D measurements.

This null hypothesis is **accepted** because there is no statistically significant difference between the direct measurement (D) and 3D measurements groups ($p > 0.05$).

- The third null hypothesis states that there is no significant difference between the 2D and 3D measurements.

This null hypothesis is **rejected** because there is a statistically significant difference between the 2D and 3D measurements ($p < 0.05$).

8. Conclusions

- A very high level of agreement was found between direct anthropometry (Gold Standard) and 3D stereo-photogrammetry.
- This study has validated the accuracy of 3D measurements versus direct measurements.
- 3D measurement techniques are more accurate, by almost 1mm in the linear diameter and up to 1 degree in angular measurements, compared to the 2D technique.

9. Recommendations

- That the 3D measurement technique could be used for improved assessment and prediction of the soft tissue changes for orthognathic surgery.

- That the 3D measurement technique could be considered a reliable method for research on soft tissue changes due to dental changes and orthopedic skeletal modification.

- That 3D images be used to help clinicians to educate their patients.

10. Appendix

Table 1: Landmarks and definitions.

Landmarks	Abbreviation	Definition
Nasion	Na	The outer point of intersection between the nasion-sella line and the soft tissue profile.
Subnasal	SubN	A point on the living where the nasal septum and the upper lip meet in the midsagittal plane
Columella	Col	The bridge of tissue that separates the nostrils at the nasal base
Pogonion	Pog	The most anterior mid- point of the chin.
Upper vermilion	UV	Upper border on upper lip vermilion
Tragus	Trg	The most posterior part of the external meatus of the ear.
Cheilion	Ch	The point located at each labial commissure.
Ala of the nose	Ala	The most lateral point on each alar contour.

Table 2 : Linear parameters and definitions.

Abbreviation	Landmarks	Definition
SbN-UV	SbN, Upper Vermelion. (mm)	Vertical linear measurement from SbN to the border of upper lip vermelion
Ch-Ch	Cheilion, right-left. (mm)	Transverse linear measurement of mouth width from Cheilion right (Ch-R), to Cheilion left (Ch-L)
Al-Al	Alare, right-left. (mm)	Transverse linear measurement of nasal width from Alare right to Alare left.
Tr-SbN	Tragus, Subnasale. (mm)	Sagittal linear measurement from Tragus to Subnasale
Tr-Pog	Tragus, Pogonion. (mm)	Sagittal linear measurement from Tragus to Pogonion
N-SbN	Nasion, Subnasale. (mm)	Vertical linear measurement of mid-face from Nasion to Subnasale
Sn-Pog	Subnasal, Pogonion. (mm)	Vertical linear measurement of lower facial dimension as measured from Subnasale to Pogonion

Table 3 : Angular parameters and definitions.

Abbreviation	Landmarks	Definition
NLA (Col-SbN-LS)	Columella. Subnasale, Labium superior (°)	Angular measurement from Columella to Subnasale to Labium superior (nasolabial angle)
N-Tr-SbN	Nasion, Tragus, Subnasale (°)	Angular measurement from Nasion to Tragus to Subnasale (angle of medium facial third)
SbN-Tr-Pog	Subnasale, Tragus, Pogonion (°)	Angular measurement from Subnasale to Tragus to Pogonion (angle of inferior facial third)
N-SbN-Pog	Nasion, Subnasale, Pogonion (°)	Angular measurement of soft tissue profile from Nasion to Subnasale to Pogonion

Table 4 : Direct Linear Measurement Data

	Sn-U Ver	Ch-Ch	Al-Al	Tr-Sn	Tr-Pog	N-Sn	Sn-Pog
A1	14.58	51.23	37.43	125.21	138.23	57.82	49.13
A2	15.66	43.43	34.47	106.37	117.22	59.23	47.32
A3	14.74	43.43	36.95	128.89	146.23	60.02	54.12
A4	12.78	49.12	40.01	138.11	149.73	63.07	49.97
A5	17.43	50.12	30.35	116.76	125.24	58.89	53.02
A6	19.12	50.54	33.23	131.32	140.32	57.21	62.18
A7	13.1	46.24	35.31	128.43	133.12	61.88	53.73
A8	19.12	5187	38.12	125.01	136.33	63.89	56.13
A9	19.32	48.23	3178	131.14	140.43	62.12	55.61
A10	12.78	50.89	34.42	128.31	137.41	51.46	51.61
A11	17.62	55.21	31.18	132.43	143.62	61	55.23
A12	14.34	52.02	40.97	129.02	145.81	59.02	63.1
A13	13.23	47.37	36.36	118.97	136.88	57.93	58.43
A14	16.98	55.03	37.67	137.43	150.23	60.89	67.33
A15	11.91	53.67	36.01	133.76	144.03	56.89	65.84
A16	12.02	55.32	35.23	124.33	143.07	56.12	50.11
A17	13.81	47.97	31.72	129.01	148.09	57.89	56.82
A18	17.96	47.34	35.87	128.22	140.86	71.01	60.38
A19	14.49	54.63	37.12	135.97	146.89	64.13	53.76
A20	15.99	44.13	32.98	126.67	138.09	61.15	65.98

A21	17.81	51.02	31.31	134.01	146.33	58.01	58.01
A22	13.43	50.64	33.29	118.76	130.59	57.31	54.2
A23	15.67	51.23	30.96	126	132.21	56.59	53.91
A24	14.81	52.55	33.12	130.01	139.98	60.34	58.97
A25	18.53	51.32	33.29	134.44	144.99	58.12	61.72
A26	13.41	49.62	33.77	132.01	141.62	61.02	61.69
A27	17.31	54.66	34.02	135.99	146.99	55.19	56.46
A28	13.56	49.23	32.18	114.31	119.69	60.52	52.39
A29	16.01	46.02	35.18	122.23	130.98	58.74	59.59
A30	15.79	45.61	37.77	126.99	140.71	69.98	63.01
A31	14.36	49.58	34.43	124	128.02	56.56	57.87
A32	15.75	46.64	30.59	121.98	135.79	55.65	52.34
A33	15.34	57.66	41.01	135.62	156.34	55.52	60.24
A34	14.98	52.12	33.56	127.21	136.69	60.99	55.23
A35	17.36	48.24	32.93	118.01	126.43	58.69	58.72
A36	12.81	50.87	31.83	124.47	136.44	53.13	59.28
A37	19.79	50.63	36.77	123.43	139.81	57.98	65.12
A38	12	48.21	35.33	122.29	133.89	54.79	50.41
A39	16.79	48.77	32	126.31	130.61	52.53	58.99
A40	16.71	46.88	28.41	120.09	132.54	56.42	56.76
A41	14.61	47.11	31.19	125.76	145.11	54.19	61.66
A42	14.73	49.59	33.13	125.97	138.02	62.97	59.02
A43	16.81	54.01	43	135.81	151.02	57.79	65.81

A44	20	52.99	38.69	129.72	141.93	60.01	69.34
A45	16.21	48.89	38.01	133.86	148.88	53.02	62.01
A46	10.17	46.32	35.23	122.42	131.44	52.79	51.32
A47	15.98	54.02	36.34	129.03	143.87	53.21	57.32
A48	14.87	44.63	32.08	120.1	131.03	57.23	60.78
A49	17.36	50.12	31.89	129.04	143.02	57.12	67.31
A50	14.21	43.02	33.26	122.78	142.69	55.02	56.26
A51	15.74	51.67	33.32	127.01	145.98	55.01	61.53

Table 5 : Direct Angular Measurement Data

	NLA	N-Tr-Sn	Sn-Tr-Pog	N-Sn-Pog
A1	122.7	26.1	24.8	164.7
A2	111.2	30.4	28.8	167.1
A3	108	27.31	24	169.8
A4	94.3	26.1	22.1	171.8
A5	113.2	28.3	29.7	162.2
A6	126.2	26	27.9	156.4
A7	111	28.4	26.3	164.2
A8	90.3	30.2	26.6	167.2
A9	124.4	27.3	25.8	160.4
A10	121.3	24.2	23.2	161.78
A11	129.3	27.1	26	154.9
A12	93.1	26.2	27.1	170.2
A13	88.1	27.9	27.4	168.3
A14	112	26.4	26.9	163
A15	116.4	24.9	29.3	152.3
A16	76.3	26.8	21.9	174.9
A17	104.9	26	23.1	175.9
A18	100	31.5	28.1	163.9
A19	102	24.9	24.5	165.1
A20	106.8	28.1	30.9	162.7
A21	106	25.7	25.6	164.9

A22	114.9	28.8	26.3	162.1
A23	131.7	26.9	24.7	157.9
A24	103.1	27.2	27.3	155.9
A25	114.5	24.8	27.1	160.5
A26	121	25.9	27.9	162
A27	120	23.9	23.7	161.6
A28	109.8	30.6	28	158.9
A29	100.1	26.2	28.3	165.8
A30	103	32.4	27.1	165.7
A31	114.9	27	27	160.1
A32	111	24.9	23.9	172.2
A33	94.1	24.6	24	168.9
A34	85	27.7	23.2	168.9
A35	101	28.5	28.3	156.9
A36	89.1	30.1	28	162.4
A37	110.1	27.5	28.5	168.2
A38	115	26	23	167
A39	118.8	24	27.8	149.9
A40	125	26.5	25.4	163
A41	102	25.4	26.7	165
A42	126.5	29.3	25	158
A43	120	25.7	25.1	162.8
A44	113.9	26.9	30.3	154.9

A45	115.5	23.7	24	161.3
A46	124.9	23.8	23.2	155.4
A47	118.4	22.8	25	157.1
A48	120.1	27	27.8	159.1
A49	133.1	25.5	28.2	154
A50	110.1	27.8	23.4	173.1
A51	121.9	24.2	25.1	163.8

Table 6 : 2D Linear Measurement Data

	Sn-U Ver	Ch-Ch	Al-Al	Tr-Sn	Tr-Pog	N-Sn	Sn-Pog
A1	14.38	50.79	36.74	124.01	137.82	58.91	47.71
A2	15.36	43.17	35.01	106.87	118.18	59.02	46.12
A3	15.22	43.13	37.11	129.17	145.21	60.07	52.79
A4	12.31	48.81	39.97	137.02	149.71	62.98	48.91
A5	16.92	49.41	31.07	115.87	125.18	58.92	52.03
A6	19.23	51.38	32.23	130.59	139.59	56.82	61.32
A7	13.79	46.82	34.91	127.03	133.71	63.01	51.89
A8	18.03	51.14	37.18	123.88	134.34	63.98	54.91
A9	18.71	47.01	32.09	129.71	139.11	62.49	53.79
A10	11.43	49.79	34.14	126.43	135.73	51.39	49.64
A11	16.07	53.72	32.01	132.02	143.05	61.76	54.23
A12	14.23	51.88	41.9	128.04	144.71	59.29	61.87
A13	11.79	46.39	35.87	117.47	134.43	57.93	57.07
A14	15.61	54.01	37.92	135.72	148.77	60.79	65.93
A15	11.25	53.11	35.97	132.46	143.14	56.97	64.63
A16	10.89	54.17	35.02	123.13	141.12	56.63	48.27
A17	12.89	47.13	32.09	127.63	146.17	58.14	55.12
A18	17.22	46.18	35.81	126.76	139.73	71.38	59.71
A19	13.78	53.49	38.04	134.77	145.72	65.11	52.91
A20	15.12	44.21	33.92	125.72	137.78	61.97	64.78
A21	17.12	51.19	32.17	132.71	145.61	57.99	57.13

A22	12.72	50.43	34.19	117.71	129.83	58.18	53.17
A23	15.01	51.17	32.18	125.07	131.72	57.03	52.71
A24	13.79	51.79	34.23	128.68	139.07	61.09	57.74
A25	18.03	50.69	34.17	133.83	144.73	59.12	60.92
A26	12.71	49.69	34.23	130.74	140.71	61.79	61.03
A27	16.83	54.48	35.12	135.27	145.81	55.98	55.83
A28	13.02	49.29	32.97	113.63	118.47	61.37	51.62
A29	15.11	44.74	36.12	121.62	129.97	59.63	58.73
A30	14.72	45.32	38.69	126.14	139.72	68.71	61.63
A31	13.72	48.82	35.73	123.07	127.64	57.73	56.49
A32	14.79	46.13	31.79	121.11	134.62	56.74	51.69
A33	14.61	57.02	41.79	134.71	155.72	56.71	59.73
A34	13.18	51.79	34.14	126.6	135.13	61.78	54.02
A35	16.12	49.01	33.82	116.79	125.11	59.89	57.16
A36	11.79	51.07	32.71	123.81	135.73	54.72	58.71
A37	18.68	50.59	37.13	122.71	138.81	59.72	64.11
A38	11.13	47.93	36.76	147.2	132.71	55.69	49.71
A39	15.82	48.16	32.73	125.63	129.64	53.81	58.62
A40	15.79	46.76	29.17	119.63	131.47	57.71	55.41
A41	13.73	46.81	32.31	124.71	144.13	55.17	60.42
A42	13.16	49.15	34.18	124.73	137.14	64.39	57.81
A43	15.63	52.98	43.79	134.81	149.67	58.82	64.19
A44	19.11	52.79	39.75	128.17	141.47	60.71	68.73

A45	15.74	49.07	38.94	132.17	147.61	53.78	60.67
A46	9.61	46.91	36.28	121.17	130.48	53.77	51.35
A47	15.61	54.72	37.17	128.71	143.18	54.79	57.27
A48	14.73	45.81	33.18	119.83	130.17	58.39	60.73
A49	17.14	51.03	33.79	128.11	143.32	58.78	66.21
A50	13.68	42.41	35.91	121.18	142.07	56.39	56.83
A51	15.79	52.15	34.93	126.71	145.79	57.16	61.47

Table 7 : 2D Angular Measurement Data

	NLA	N-Tr-Sn	Sn-Tr-Pog	N-Sn-Pog
A1	123.1	25.9	24.7	161.8
A2	111.3	30.3	28	165.4
A3	108.9	27.4	24.9	168.7
A4	94.4	26.7	22.7	171
A5	113.3	28.3	29.9	160.3
A6	126.4	26.4	28.3	154.3
A7	113.7	28.7	25.9	162.7
A8	90.6	30.7	26.7	165.3
A9	124.3	27.9	26.9	158.7
A10	121.7	25.2	24.8	161.9
A11	130.3	26.9	26.3	153.7
A12	93.7	26.3	28.7	168.6
A13	87.9	28.6	27.4	166.4
A14	112.7	26.7	28.9	161.7
A15	116.4	25.6	29.4	150.3
A16	77.3	27.3	22.9	174.3
A17	105.9	26.8	24.6	174.2
A18	101.6	32.7	28.7	163.4
A19	102.4	26.3	25.7	164.3
A20	107.3	28.4	31.4	161.2
A21	106.7	26.6	26.6	164.1

A22	115.7	29.9	27.8	160.7
A23	131.9	26.9	25.4	157.1
A24	103.3	28.3	28.3	154.3
A25	115.6	25.7	28.7	159.1
A26	121.3	27.3	29.3	160.7
A27	120.4	25.6	24.9	160.3
A28	110.7	31.3	28.3	158.4
A29	101.9	27.4	28.9	165.4
A30	103.2	33.7	28.4	164.3
A31	116.7	27.4	27.7	158.7
A32	111.8	26.7	24.7	171.1
A33	94.7	25.6	24.8	167.7
A34	86.4	28.7	24.9	168.1
A35	101.3	29.6	29.7	157.8
A36	89.9	30.2	29.9	161.3
A37	111.4	28.7	29.8	167.2
A38	115.3	27.4	23.7	165.3
A39	119.7	24.6	28.3	149.1
A40	125.7	27.8	26.3	161.7
A41	103.4	26.7	27.4	164.1
A42	127.3	30.7	26.7	157.3
A43	120.7	26.3	26.7	161.3
A44	114.6	28.6	31.6	153.7

A45	116.6	24.7	25.3	160.4
A46	126.3	26.1	25.3	155.1
A47	120.4	24.7	26.2	156.3
A48	120.4	28.3	28.4	157.2
A49	133.1	26.7	28.3	153.5
A50	110.7	28.2	25.7	171.3
A51	122.7	26.3	27.2	162.1

Table 8 : 3D Linear Measurement Data

	Sn-U Ver	Ch-Ch	Al-Al	Tr-Sn	Tr-Pog	N-Sn	Sn-Pog
A1	14.88	50.84	36.39	124.74	138.6	58.48	48.22
A2	15.99	43.19	34.24	107.1	118.9	58.35	46.62
A3	15.53	43.23	36.66	129.97	146.8	59.56	53.39
A4	12.96	48.88	39.03	137.8	150.19	62.04	49.33
A5	17.66	49.3	30.45	116.2	126.05	57.84	52.83
A6	19.24	51.4	32.26	130.58	139.57	56.82	61.35
A7	13.88	47.48	34.92	127.64	134.12	61.78	52.96
A8	18.36	51.26	37.79	124.44	135.64	63.16	55.96
A9	18.74	47.83	31.58	130.39	139.84	61.37	54.47
A10	12.06	50.38	33.85	127.2	136.27	50.98	50.38
A11	16.59	54.29	31.28	132.23	143.51	60.9	55.11
A12	14.21	51.93	40.9	128.98	145.1	58.09	62.72
A13	12.64	46.34	35.27	118.37	135.69	57.02	57.82
A14	16.22	54.15	37.24	136.32	149.19	60.08	66.81
A15	11.8	53.23	35.34	133.22	143.54	56.01	65.13
A16	11.42	54.95	34.14	123.89	142.5	55.39	49.16
A17	13.58	48.3	31.55	128.29	147.89	57.26	56.06
A18	18.16	47.11	35.26	127.99	140.67	70.59	60.3
A19	14.4	53.52	37.09	135.48	146.36	64.08	53.46
A20	15.63	44.2	33.1	126.1	138.32	61.12	65.55
A21	17.77	51.24	31.29	133.51	146.53	57.74	58.01

A22	13.38	50.49	33.24	118.65	130.54	57.22	54.24
A23	15.58	51.2	31.17	125.95	132.44	56.54	53.88
A24	14.87	52.5	33.79	129.78	140.14	60.28	58.36
A25	18.49	51.58	33.27	134.46	145.22	58.02	61.69
A26	13.39	49.73	33.77	131.89	141.48	60.98	61.63
A27	17.25	54.58	34.06	136.17	146.97	55.14	56.41
A28	13.58	49.41	32.16	114.24	119.66	60.46	52.4
A29	15.91	45.99	35.14	122.14	130.82	58.71	59.57
A30	15.71	45.58	37.77	127.11	140.72	69.45	62.88
A31	14.58	49.6	34.46	123.98	128.26	56.41	57.6
A32	15.57	46.61	30.5	122.04	135.73	55.42	52.36
A33	15.48	57.86	40.98	135.5	156.26	55.47	60.21
A34	14.8	52.04	33.58	127.19	136.68	60.97	55.21
A35	17.31	48.28	32.93	117.84	126.49	58.76	58.72
A36	12.88	50.92	31.62	124.41	136.66	53.67	59.2
A37	19.74	50.6	36.72	123.14	139.74	58.84	65.07
A38	12	48.17	35.32	122.2	133.8	54.88	50.38
A39	16.85	48.56	31.93	126.1	130.59	52.65	59.08
A40	16.64	46.86	28.36	120.14	132.87	56.46	56.59
A41	14.59	47.09	31.21	125.6	145.02	54.14	61.63
A42	14.82	49.55	33.26	125.78	138.31	63.26	58.96
A43	16.73	53.86	42.99	135.76	150.99	57.8	65.77
A44	20.06	53.04	38.63	129.67	142.03	59.03	69.27

A45	16.18	48.83	37.86	133.64	148.84	52.89	61.99
A46	10.13	46.7	35.15	122.39	131.36	52.67	52.44
A47	16.76	54.41	36.93	129.98	144.65	53.4	58.48
A48	15.22	44.77	32.3	120.93	131.35	57.76	61.17
A49	18.2	50.24	32.42	129.72	144.03	57.3	67.44
A50	14.77	43.31	34.77	123.22	143.03	55.94	57.9
A51	16.11	52.85	33.84	127.91	146.91	56.06	62.74

Table 9 : 3D Angular Measurement Data

	NLA	N-Tr-Sn	Sn-Tr-Pog	N-Sn-Pog
A1	122.2	25.7	24	162.9
A2	110.7	29.9	27.6	166
A3	107.2	26.9	23.2	169.9
A4	93.1	25.8	21.5	171.2
A5	112.7	27.7	29	161.7
A6	125.2	25.2	27.2	155.7
A7	112.2	27.8	25.1	163.4
A8	89.2	29.3	25.8	166.1
A9	123.8	27	25.2	159.7
A10	120.3	24	23.9	162.1
A11	129	26.2	25.4	154.4
A12	92.8	25.8	27.5	169.3
A13	87.4	27.2	26.7	167.7
A14	111.3	25.9	27.5	162.1
A15	115.6	24.4	28.9	151.8
A16	76.7	26.5	22	174.9
A17	105	25.7	23.5	175.6
A18	100.5	31.1	27.9	164
A19	101.3	25.1	24.8	165.1
A20	106	27.7	30.6	162.1
A21	105.6	25.8	25.4	165

A22	114.5	28.4	26.7	161.9
A23	131.2	26.5	24.8	158.3
A24	102.9	27	27.3	155.8
A25	114.4	24.5	27.5	160.3
A26	120.7	26.4	28.1	161.9
A27	119.8	24.1	23.7	161.7
A28	109.3	30.4	27.7	159.2
A29	100.4	26.8	27.8	165.7
A30	102.5	32.3	27.3	165.6
A31	115.3	26.9	26.6	159.8
A32	111	25.1	23.8	172.3
A33	94.1	24.5	23.9	168.3
A34	85.5	27.6	23.5	169
A35	100.8	28.5	28.3	156.6
A36	89	29.9	28.01	162.9
A37	110.7	27.3	28.3	168.4
A38	114.9	26	22.9	166.8
A39	118.4	23.8	27.8	150.2
A40	124.6	26.3	25.4	162.8
A41	102.7	25.3	26.3	165.2
A42	126.6	29.2	25.1	158
A43	119.3	25.4	25.3	162.5
A44	113.3	27.2	30.7	154.8

A45	115.5	23.4	24	161.6
A46	125.6	24.6	24.2	156.7
A47	119.6	23.5	25.1	157.9
A48	119.3	27.1	27.3	158.7
A49	132.5	25.5	27.8	154.1
A50	109.3	27.5	24	172.8
A51	121.1	25.6	26.4	163.4

Table 10 : Data of Randomly Selected Subjects

		10% Random selected subjects										
		Sn-U Ver	Ch-Ch	Al-Al	Tr-Sn	Tr-Pog	N-Sn	Sn-Pog	NLA	N-Tr-Sn	Sn-Tr-Pog	N-Sn-Pog
A3	**D**	14.84	43.63	37.06	128.93	146.33	60.16	54.03	108	27.2	24.3	169.7
A20	**D**	16.19	44.33	33.11	126.66	138.18	61.19	65.83	107	28	31	161.9
A32	**D**	15.95	46.58	30.73	121.92	135.81	55.59	52.44	111.2	25.1	24.1	172.9
A41	**D**	14.81	47.21	31.41	125.76	145.19	54.23	61.63	102.3	25.9	26.9	165.4
A51	**D**	15.71	51.72	33.64	127.21	146.08	55.21	61.57	122.1	24.2	25.4	163.1
A3	**D2**	15.32	43.24	37.47	129.27	145.41	60.09	52.68	108.9	27.4	24.9	167.9
A20	**D2**	15.82	44.29	34.12	125.84	137.88	61.77	64.75	106.3	28.4	31.6	161.9
A32	**D2**	14.82	46.24	31.88	121.21	134.69	56.79	51.71	112	26.7	24.4	171.8
A41	**D2**	13.91	46.95	32.46	124.79	144.23	55.23	60.39	103.4	26.7	27.9	163.8
A51	**D2**	15.94	52.23	35.09	126.68	145.67	57.19	61.47	122.7	26.3	26.9	162.6
A3	**D3**	15.56	43.34	36.81	129.47	146.91	59.61	53.39	108	27.3	23.9	170
A20	**D3**	15.69	44.26	33.19	126.11	138.38	61.13	65.54	107	27.9	30.8	162.1
A32	**D3**	15.61	46.72	30.61	122.09	135.69	55.44	52.38	111	25.3	24.5	172.3
A41	**D3**	14.63	47.13	31.63	125.66	144.91	54.12	61.61	102.7	25.6	26.3	165.2
A51	**D3**	16.18	52.87	33.91	127.99	146.87	56.1	62.74	121.3	25.4	25.9	163.7

Ethics Approval

UNIVERSITY OF MANITOBA | Research Ethics and Compliance

Research Ethics - Bannatyne
P126-770 Bannatyne Avenue
Winnipeg, MB
Canada R3E 0W3
Phone +204-789-3255
Fax +204-789-3414

HEALTH RESEARCH ETHICS BOARD (HREB)
CERTIFICATE OF FINAL APPROVAL FOR NEW STUDIES
Full Board Review

PRINCIPAL INVESTIGATOR: Dr. Amin Neishaboory	**INSTITUTION/DEPARTMENT:** U of M/Dentistry/Orthodontics	**ETHICS #:** HS21427 (H2018:008)
HREB MEETING DATE: January 22, 2018	**APPROVAL DATE:** February 5, 2018	**EXPIRY DATE:** **January 22, 2019**
STUDENT PRINCIPAL INVESTIGATOR SUPERVISOR (If applicable): Dr. Robert Drummond		

PROTOCOL NUMBER: NA	**PROJECT OR PROTOCOL TITLE:** Validity and comparison between 2D (Normal Photo) and 3dMD (3D image) in Orthodontic diagnosis
SPONSORING AGENCIES AND/OR COORDINATING GROUPS: NA	

Submission Date(s) of Investigator Documents: December 12, 2017 and February 1, 2018 (Received)	**REB Receipt Date(s) of Documents:** December 12, 2017 and February 1, 2018

THE FOLLOWING ARE APPROVED FOR USE:

Document Name	Version(if applicable)	Date
Protocol:		
Proposal submitted February 1, 2018		
Consent and Assent Form(s):		
Consent Disclosure Statement	V. 2	31 Jan 2018
Other:		
Table 1 - Land Marks (Undated)		submitted February 1, 2018
Table 2 - Angular and Linear Measurements (Undated)		submitted February 1, 2018

CERTIFICATION

The University of Manitoba (UM) Health Research Board (HREB) has reviewed the research study/project named on this ***Certificate of Final Approval*** at the ***full board meeting*** date noted above and was found to be acceptable on ethical grounds for research involving human participants. The study/project and documents listed above was granted final approval by the Chair or Acting Chair, UM HREB.

HREB ATTESTATION
The University of Manitoba (UM) Health Research Board (HREB) is organized and operates according to Health Canada/ICH Good Clinical Practices, Tri-Council Policy Statement 2, and the applicable laws and regulations of Manitoba. In respect to clinical trials, the HREB complies with the membership requirements for Research Ethics Boards defined in Division 5 of the Food and Drug Regulations of Canada and carries out its functions in a manner consistent with Good Clinical Practices.

QUALITY ASSURANCE
The University of Manitoba Research Quality Management Office may request to review research documentation from this research study/project to demonstrate compliance with this approved protocol and the University of Manitoba Policy on the Ethics of Research Involving Humans.

CONDITIONS OF APPROVAL:
1. The study is acceptable on scientific and ethical grounds for the ethics of human use only. ***For logistics of performing the study, approval must be sought from the relevant institution(s).***
2. This research study/project is to be conducted by the local principal investigator listed on this certificate of approval.
3. The principal investigator has the responsibility for any other administrative or regulatory approvals that may pertain to the research study/project, and for ensuring that the authorized research is carried out according to governing law.
4. **This approval is valid until the expiry date noted on this certificate of approval.** **A Bannatyne Campus Annual Study Status Report** must be submitted to the REB within 15-30 days of this expiry date.
5. Any changes of the protocol (including recruitment procedures, etc.), informed consent form(s) or documents must be reported to the HREB for consideration in advance of implementation of such changes on the **Bannatyne Campus Research Amendment Form.**
6. Adverse events and unanticipated problems must be reported to the REB as per Bannatyne Campus Research Boards Standard Operating procedures.
7. The UM HREB must be notified regarding discontinuation or study/project closure on the **Bannatyne Campus Final Study Status Report**.

Sincerely,

[redacted]

Bannatyne Campus

Please quote the above Human Ethics Number on all correspondence.
Inquiries should be directed to the REB Secretary **Telephone:** (204) 789-3255/ **Fax:** (204) 789-3414

Consent Form

University of Manitoba Bannatyne Campus Research Ethics Board
Consent Disclosure Statement

Validity and comparison between 2D (Normal Photo) and 3dMD (3D image) in Orthodontic diagnosis

Thank you for your interest in participating in this clinical study. Dr. Amin Neishaboory is a master of dentistry Orthodontic resident and in his role as the Principal Investigator for this trial he will be collecting data in the form of taking two sets of facial 2D and 3D photographs in on session. (around 15min in total)

This study is being conducted to establish the reliability and comparison of 2D and 3D photo analysis in some linear and angular measurements for Orthodontic treatment planning.

Your participation on this research project is completely voluntary. You are not required to provide any personal information such as your name, address or telephone number, and you don't have to answer any questions.

In this project, we need to take 2 sets of photos (Ordinary camera and 3dMD machine, no x-ray involved) which may take around 15 min in total for both sets in one session. (Time can be arranged) Then we perform some measurements on some selected land marks on the photos and compare them together.

The risks of participating are low, as no x-ray would be involved. Your photos will remain confidential with no personal data/information collected or attached to the photos on a file with secure password (only accessible by Dr.Amin Neishaboory and Dr.Robert Drummond) in orthodontic department of university of Manitoba, however, your photos maybe be used in scientific/training presentations. (Just photos without any personal information),You have the right to NOT give us the permission to use the photos in presentations but still may be happy to allow us using them in this project for the measurements purposes only.

In this project, we are happy to compensate the time that you will allocate for participation in this project with a $10 Gift Card at the end of the photo shooting session.

Your participation is not only important to us but also will be appreciated with future patients who would benefit from the more accurate and less invasive diagnostic tool for their orthodontic treatment. If you have any questions or concerns about this study or participation in it, please do not hesitate to contact Dr. Amin Neishaboory at 204-915-7277.

This study has been approved by the University of Manitoba Health Research Ethics Board.

I consent to participate in this study.	○ Yes	○ No
I give permission to use my photos for scientific/training purposes.	○ Yes	○ No
I give permission to use my photos for presentation purposes.	○ Yes	○ No

Participant Full Name (Print): Participant (Signature/Date):

Witness (Print): Witness(Signature):

31 Jan 2018-Ver.2

11.Refrences

Ackerman, JL, WR Proffit, and DM Sarver. 1999. “The Emerging Soft Tissue Paradigm-Ack,Prof,Sarv.Pdf.” *Clin. Orth. Res.*

Arnett, G. William, and Robert T. Bergman. 1993. “Facial Keys to Orthodontic Diagnosis and Treatment Planning. Part I.” *American Journal of Orthodontics and Dentofacial Orthopedics* 103 (4). Elsevier: 299–312. doi:10.1016/0889-5406(93)70010-L.

Brons, Sander, Machteld E. van Beusichem, Ewald M. Bronkhorst, Jos Draaisma, Stefaan J. Bergé, Thomas J. Maal, and Anne Marie Kuijpers-Jagtman. 2012. “Methods to Quantify Soft-Tissue Based Facial Growth and Treatment Outcomes in Children: A Systematic Review.” Edited by Arin Greene. *PLoS ONE* 7 (8). Public Library of Science: e41898. doi:10.1371/journal.pone.0041898.

Chae, Michael P, Warren Matthew Rozen, Robert T Spychal, and David J Hunter-smith. 2016. “Breast Volumetric Analysis for Aesthetic Planning in Breast Reconstruction : A Literature Review of Techniques.” *Gland Surg.* 5 (2): 212–26. doi:10.3978/j.issn.2227-684X.2015.10.03.

Deli, Roberto, L M Galantucci, Alberto Laino, Raoul D’Alessio, E D Gioia, Carmela Svastano, Fulvio Lavecchia, and Gianluca Percoco. 2013. “Three-Dimensional Methodology for Photorammetric Acquisition of the Soft Tissues of the Face: New Clinical-Instrumental Protocol.” *Progress in Orthodontics* 14 (1): 32. doi:10.1186/2196-1042-14-32.

Dindaroğlu, Furkan, Pinar Kutlu, Gökhan Serhat Duran, Serkan Görgülü, and Erhan Aslan. 2016. “Accuracy and Reliability of 3D Stereophotogrammetry: A Comparison to Direct Anthropometry and 2D Photogrammetry.” *Angle Orthodontist* 86 (3): 487–94. doi:10.2319/041415-244.1.

Forst, Darren, Simrit Nijjar, Carlos Flores-Mir, Jason Carey, Marc Secanell, and Manuel Lagravere. 2014. “Comparison of in Vivo 3D Cone-Beam Computed Tomography Tooth Volume Measurement Protocols.” *Progress in Orthodontics* 15: 69. doi:10.1186/s40510-014-0069-2.

Galantucci, L. M., R. Ferrandes, and G. Percoco. 2006. “Digital Photogrammetry for Facial Recognition.” *Journal of Computing and Information Science in Engineering* 6 (4): 390. doi:10.1115/1.2356499.

Ghoddousi, H., R. Edler, P. Haers, D. Wertheim, and D. Greenhill. 2007. “Comparison of Three Methods of Facial Measurement.” *International Journal of Oral and Maxillofacial Surgery* 36 (3): 250–58. doi:10.1016/j.ijom.2006.10.001.

Hellak, Andreas F, Bernhard Kirsten, Michael Schauseil, Rolf Davids, Wolfgang M Kater, and Heike M Korbmacher-Steiner. 2015. “Influence of Maxillary Advancement Surgery on Skeletal and Soft-Tissue Changes in the Nose - a Retrospective Cone-Beam Computed Tomography Study.” *Head & Face Medicine* 11. Head & Face Medicine: 23. doi:10.1186/s13005-015-0080-y.

Khambay, B., N. Nairn, A. Bell, J. Miller, A. Bowman, and A. F. Ayoub. 2008. “Validation and Reproducibility of a High-Resolution Three-Dimensional Facial Imaging System.” *British Journal of Oral and Maxillofacial Surgery* 46 (1): 27–32. doi:10.1016/j.bjoms.2007.04.017.

Kochel, Janka, Philipp Meyer-Marcotty, Michael Kochel, Susanne Schneck, and Angelika Stellzig-Eisenhauer. 2010. “3D Soft Tissue Analysis--Part 2: Vertical Parameters.” *Journal of Orofacial Orthopedics = Fortschritte Der Kieferorthopädie : Organ/Official Journal Deutsche Gesellschaft Für Kieferorthopädie* 71 (3): 207–20. doi:10.1007/s00056-010-9943-9.

Lane, Christopher, and William Harrell. 2008. “Completing the 3-Dimensional Picture.” *American Journal of Orthodontics and Dentofacial Orthopedics* 133 (4). Elsevier: 612–20. doi:10.1016/j.ajodo.2007.03.023.

Lübbers, Heinz Theo, Laurent Medinger, Astrid Kruse, Klaus Wilhelm Grätz, and Felix Matthews. 2010. “Precision and Accuracy of the 3dmd Photogrammetric System in Craniomaxillofacial Application.” *Journal of Craniofacial Surgery* 21 (3): 763–67. doi:10.1097/SCS.0b013e3181d841f7.

Maués, C.P.R., M.V.S. Casagrande, R.C.C. Almeida, M.A.O. Almeida, and F.A.R. Carvalho. 2018. “Three-Dimensional Surface Models of the Facial Soft Tissues Acquired with a Low-Cost Scanner.” *International Journal of Oral and Maxillofacial Surgery*, April. Churchill Livingstone. doi:10.1016/J.IJOM.2018.03.028.

Naini, Farhad B., Sarah Akram, Julia Kepinska, Umberto Garagiola, Fraser McDonald, and David Wertheim. 2017. “Validation of a New Three-Dimensional Imaging System Using Comparative Craniofacial Anthropometry.” *Maxillofacial Plastic and Reconstructive Surgery* 39 (1). Maxillofacial Plastic and Reconstructive Surgery: 23. doi:10.1186/s40902-017-0123-3.

Nanda, Vikrum, Boris Gutman, Ehab Bar, Suha Alghamdi, Sotirios Tetradis, Aldons J. Lusis, Eleazar Eskin, and Won Moon. 2015. “Quantitative Analysis of 3-Dimensional Facial Soft Tissue Photographic Images: Technical Methods and Clinical Application.” *Progress in Orthodontics* 16 (1). Progress in Orthodontics: 1–9. doi:10.1186/s40510-015-0082-0.

Proffit, WR, HW Fields, and DM Sarver. 2015. “Contemporary Orthodontics.” In *St Louis*. doi:10.1038/sj.bdj.2012.829.

Rangel, Frits A., T. J J Maal, Stefaan J. Bergé, O. J C van Vlijmen, Joanneke M. Plooij, Filip

Schutyser, and Anne Marie Kuijpers-Jagtman. 2008. “Integration of Digital Dental Casts in 3-Dimensional Facial Photographs.” *American Journal of Orthodontics and Dentofacial Orthopedics* 134 (6). American Association of Orthodontists: 820–26. doi:10.1016/j.ajodo.2007.11.026.

Schimmel, Martin, Panagiotis Christou, Odyssia Houstis, François R. Herrmann, Stavros Kiliaridis, and Frauke Müller. 2010. “Distances between Facial Landmarks Can Be Measured Accurately with a New Digital 3-Dimensional Video System.” *American Journal of Orthodontics and Dentofacial Orthopedics* 137 (5): 1–10. doi:10.1016/j.ajodo.2009.03.039.

Swennen, G.R.J., F. Schutyser, A. Lemaitre, C. Malevez, and A. De Mey. 2005. “Accuracy and Reliability of 3-D CT versus 3-D Stereo Photogrammetry Based Facial Soft Tissue Analysis.” *International Journal of Oral and Maxillofacial Surgery* 34: 73. doi:10.1016/S0901-5027(05)81161-0.

Tzou, C H, and M Frey. 2011. “Evolution of 3D Surface Imaging Systems in Facial Plastic Surgery.” *Facial Plast Surg Clin North Am* 19 (4). Elsevier Inc: 591–602, vii. doi:10.1016/j.fsc.2011.07.003.

Winder, R. J., T. A. Darvann, W. McKnight, J. D M Magee, and P. Ramsay-Baggs. 2008. “Technical Validation of the Di3D Stereophotogrammetry Surface Imaging System.” *British Journal of Oral and Maxillofacial Surgery* 46 (1): 33–37. doi:10.1016/j.bjoms.2007.09.005.

Wong, Julielynn Y., Albert K. Oh, Eiichi Ohta, Anne T. Hunt, Gary F. Rogers, John B. Mulliken, and Curtis K. Deutsch. 2008. “Validity and Reliability of Craniofacial Anthropometric Measurement of 3D Digital Photogrammetric Images.” *Cleft Palate-*

Craniofacial Journal 45 (3): 232–39. doi:10.1597/06-175.